Received: 12 August 2020 | Revised: 26 November 2020 | Accepted: 30 November 2020

DOI: 10.1002/glia.23950

GLIA

WILEY

RESEARCH ARTICLE

Beneficial contribution of induced pluripotent stem cell-progeny to Connexin 47 dynamics during demyelination-remyelination

Sabah Mozafari[1,2,3,4] | Cyrille Deboux[1,2,3,4] | Cecilia Laterza[5,8] | Marc Ehrlich[6,7] | Tanja Kuhlmann[7] | Gianvito Martino[5] | Anne Baron-Van Evercooren[1,2,3,4]

[1]INSERM, U1127, Paris, France

[2]CNRS, UMR 7225, Paris, France

[3]Sorbonne Université UPMC Paris 06, UM-75, Paris, France

[4]ICM-GH Pitié-Salpêtrière, Paris, France

[5]Institute of Experimental Neurology-DIBIT 2, Division of Neuroscience, IRCCS San Raffaele Hospital and Vita San Raffaele University, Milan, Italy

[6]Department of Cell and Developmental Biology, Max Planck Institute for Molecular Biomedicine, Münster, Germany

[7]Institute of Neuropathology, University Hospital Münster, Münster, Germany

[8]Industrial Engineering Department, University of Padova, Padova, Italy

Correspondence
Sabah Mozafari, Institut du Cerveau et de la Moelle, 47 Bv de l'Hôpital, Paris 75013, France.
Email: sabah.mozafari@icm-institute.org

Funding information
Progressive MS Alliance (PMSA) Collaborative Research Network, Grant/Award Number: PA-1604-08492 (BRAVEinMS); European Committee for Treatment and Research in Multiple Sclerosis (ECTRIMS); INSERM and ICM Internal Fundings; Italian Multiple Sclerosis Foundation (FISM); National MS Society, Grant/Award Number: NMSS RG-1801-30020

Abstract

Oligodendrocytes are extensively coupled to astrocytes, a phenomenon ensuring glial homeostasis and maintenance of central nervous system myelin. Molecular disruption of this communication occurs in demyelinating diseases such as multiple sclerosis. Less is known about the vulnerability and reconstruction of the panglial network during adult demyelination-remyelination. Here, we took advantage of lysolcithin-induced demyelination to investigate the expression dynamics of the oligodendrocyte specific connexin 47 (Cx47) and to some extent that of astrocyte Cx43, and whether this dynamic could be modulated by grafted induced pluripotent stem cell (iPSC)-neural progeny. Our data show that disruption of Cx43-Cx47 mediated heterocellular gap-junction intercellular communication following demyelination is larger in size than demyelination. Loss of Cx47 expression is timely rescued during remyelination and accelerated by the grafted neural precursors. Moreover, mouse and human iPSC-derived oligodendrocytes express Cx47, which co-labels with astrocyte Cx43, indicating their integration into the panglial network. These data suggest that in rodents, full lesion repair following transplantation occurs by panglial reconstruction in addition to remyelination. Targeting panglial elements by cell therapy or pharmacological compounds may help accelerating or stabilizing re/myelination in myelin disorders.

KEYWORDS

Connexin 43, Connexin 47, demyelination, iPSC-neural precursors, oligodendrocytes, panglial repair, remyelination, transplantation

1 | INTRODUCTION

In the central nervous system (CNS), remyelination of adult axons provides trophic support, rescues loss of function, and protects neurons from subsequent axonal degeneration. While remyelination can be provided by endogenous or exogenous progenitors, stem cells, and especially induced pluripotent stem cell (iPSC) derived neural precursors (NPCs) or oligodendrocyte progenitors (OPCs) have become

attractive candidates to promote CNS remyelination (Chanoumidou, Mozafari, Baron-Van Evercooren, & Kuhlmann, 2020; Mozafari & Baron-Van Evercooren, 2020). In particular, intraparenchymal engraftment of mouse and human iPSCs-NPCs or -OPCs in adult demyelinating conditions results in functional remyelination of host axons (Ehrlich et al., 2017; Mozafari et al., 2015). Grafted NPCs may also provide neuroprotection via trophic support and/or immunomodulation (Ottoboni, von Wunster, & Martino, 2020; Pluchino, Smith, & Peruzzotti-Jametti, 2020). As far as cell replacement is concerned, integration of the grafted cells has been evaluated essentially based on their ability to interact with host axons and reconstruct myelin (axo-glial interactions). However, their capacity to interact with other glial cells (glial-glial interactions) in order to participate in the pan glial network has been overlooked. This is of major importance since glial-glial interactions are essential for myelin maintenance (Tress et al., 2012) and full repair. Moreover, less is known about how to protect or accelerate panglial repair following adult demyelination.

Astrocytes play an important role in facilitating myelination and myelin maintenance by clearance of extracellular ions and neurotransmitters and by secretion of nutrients including pro-myelinating factors in the CNS (Claycomb, Johnson, Winokur, Sacino, & Crocker, 2013; Li, Giaume, & Xiao, 2014). Thus, oligodendrocytes are dependent upon astrocytes for their vital functions and this is primarily controlled by gap junction (GJ) connections. Astrocyte-oligodendrocyte coupling via GJs is crucial for both myelin formation and maintenance, due to K^+ buffering, energy, and metabolic support for oligodendrocytes via the panglia syncytium (Basu & Sarma, 2018).

In the CNS, the three macroglial cell types, astrocytes, oligodendrocytes, and ependymocytes, are extensively interconnected by GJs channels to form a panglial syncytium. Each of these cells express a set of cell-specific connexins that can connect to form autologous or heterologous GJs (Orthmann-Murphy, Abrams, & Scherer, 2008). Oligodendrocytes specifically express Cx47, Cx32, Cx45, and Cx29 while astrocytes express mainly Cx43, Cx30, and Cx26. Oligodendrocytes, as part of the glial syncytium, are extensively coupled to astrocytes through heterologous GJs such as Cx47/Cx43 and Cx32/Cx30. Cx47/Cx43 channels are largely localized to the oligodendrocyte somata, where they outnumber Cx32/Cx30 channels (Altevogt & Paul, 2004; Kamasawa et al., 2005; Kleopa, Orthmann, Enriquez, Paul, & Scherer, 2004; Nagy, Ionescu, Lynn, & Rash, 2003).

Several in vitro and in vivo studies highlighted that Cx43/Cx47 channels are of major importance for astrocyte/oligodendrocyte crosstalk. It has been proposed that depletion of either Cx43 or Cx47 affects the maintenance of white matter function via alterations in astrocyte-oligodendrocyte homeostasis and plays a key role in chronic expansion of demyelinated plaques (Basu & Sarma, 2018). Molecular disruption of astrocytes/oligodendrocytes communication (loss of Cx43/Cx47 connectivity) occurs in demyelinating diseases such as multiple sclerosis (MS) (Markoullis et al., 2014; Masaki, 2015; Masaki et al., 2013; Rash, 2010). Loss of Cx43 in astrocytes is directly correlated with the extent of demyelination and severity of disease in MS and neuromyelitis optica (NMO). Moreover, extensive loss of Cx43 in the lesion is related to frequent of relapses and rapid disease course (Masaki et al., 2013). While immunoreactivity for astrocyte Cx43 is completely lost within active MS and NMO, it is upregulated in chronic lesions (Masaki et al., 2013). A significant reduction of astrocyte Cx43, specifically in monocyte infiltrated areas, and a reduction of oligodendrocyte Cx47 in and around the demyelinated plaques occur also in experimental autoimmune encephalomyelitis (EAE; Brand-Schieber et al., 2005). However, the mechanism of GJ expression alteration in oligodendrocytes has not been investigated. In fact, whether demyelinating diseases such as MS with repeated episodes of demyelination could be a cause or a consequence of panglial network deconstruction is not clear.

Genetic alterations of oligodendrocyte or astrocyte connexins lead to myelin disorders. Mutations in the GJC2 gene encoding for human Cx47 cause the hypomyelinating leukodystrophy Pelizaeus–Merzbacher-like disease. In addition, mutations in the GJB1 gene encoding Cx32 result in the demyelinating neuropathy X-linked Charcot–Marie–Tooth disease, which can be associated with CNS abnormalities (Kleopa & Scherer, 2006; Uhlenberg et al., 2004). Cx47 genetic ablation in rodents can significantly abolish oligodendrocytes-astrocytes coupling, with the number of coupled oligodendrocytes being reduced by 80% (Maglione et al., 2010), suggesting a major role for connexin-mediated GJs in oligodendrocyte homeostasis and developmental myelination. Moreover, Cx47 ablation results in myelination abnormalities in and around the compact myelin or peri-axonal space and conspicuous vacuolation of nerve fibers in white matter regions. These pathological features are worsened by double deletion of Cx32 and Cx47 resulting in severe myelin alterations and death of the animals (Odermatt et al., 2003). MHV-A59 infection leads to a small, but significant, and persistent downregulation of Cx47 in the MHV-A59 infected brain, and persistent alteration of Cx47 is associated with the loss of the myelin marker PLP in the major white matter tracts of the brain (Basu, Bose, Thomas, & Das Sarma, 2017). It has been hypothesized that Cx47 gene mutations affects the permeability of Cx47 channels, which in turn alters exchange of substances between oligodendrocytes or astrocytes, and the way that glia support myelin function (Fasciani et al., 2018). Finally, oligodendrocyte-specific conditional ablation of Cx47 exacerbates acute and chronic relapsing EAE (Zhao et al., 2020). These evidences suggest that oligodendrocyte Cx47 and/or its astrocyte Cx43 counterpart play an important role in remyelination or myelin pathology. So far, only one study reported the dynamic expression pattern of Cx47 in a cuprizone-induced demyelination mouse model (Parenti et al., 2010). However, how oligodendrocytes lose and gain Cx47 or Cx43 expression and whether the panglial repair can be accelerated was not addressed.

We reported previously that following lysolecithin (LPC)-induced adult demyelination, grafted iPSC-NPCs/OPCs timely differentiate into oligodendrocytes (but also ~20% to astrocytes), and extensively remyelinate the lesion 6 weeks (rodent cells) or 12 weeks (human cells) after engraftment (Ehrlich et al., 2017; Mozafari et al., 2015; Mozafari et al., 2020). However, the timing and dynamics of loss and gain of Cx47 expression during demyelination and remyelination, and the potential interaction of the iPSC-derived oligodendrocytes (through the connexins) with astrocytes during this successful remyelination has not been addressed. Here, we studied in detail the

dynamics of Cx47 expression by endogenous and exogenous oligodendrocytes during the demyelination-remyelination process. The expression changes in Cx43 levels were also assessed. We find that LPC-induced demyelination causes the loss of the panglial network. While endogenous and exogenous myelinating oligodendrocytes express Cx47 and contribute to the panglial network reconstruction in response to demyelination, exogenous oligodendrocytes accelerate the panglial repair.

2 | MATERIALS AND METHODS

2.1 | Cell culture

2.1.1 | Mouse iPSC-NPCs

miPSCs were generated from reprogrammed E14.5 C57Bl/6 *Sox2*$^{ßgeo/ßgeo}$ knock-in embryonic fibroblasts expressing a ßgeo cassette under the control of the Sox2 promoter that provides cell resistance to neomycin (Laterza et al., 2013). NPCs were grown in uncoated plastic flasks (T75) in Euromed-N medium (Euroclone) supplemented with 1% N2 nutrients (Invitrogen), Pen/strep (Invitrogen), L-glutamine (200 nM) (Invitrogen) and 20 ng/ml basic fibroblast growth factor (Preprotech) and 20 ng/ml epidermal growth factor (EGF) (Preprotech). Fresh medium was added every other day. Cells were split once a week depending on cell density and were reseeded at a density of 10^6 cells/T75 flask in 10 ml of medium.

2.1.2 | Mouse embryonic NPCs

Primary mouse NPCs were obtained from E12/E13 C57Bl/6 mice as previously described (Deboux et al., 2013). Briefly, brains were dissected free of meninges, dissociated using ATV (0.05% trypsin, 0.1% glucose and 0.5 nM EDTA). Collected cells were resuspended in NEF medium composed of DMEM/F12 medium (1:1) supplemented with N2 nutrients (1%), B27 (0.5%), insulin (25 μg/ml), glucose (6 mg/ml), Hepes (5 mM), FGF2 (20 ng/ml), and EGF (20 ng/ml). NPCs were dissociated once a week and reseeded at the density of 10^6 cells/T75 flask in 10 ml medium. Immunocytochemistry showed that miPS-NPCs similar to their embryonic counterparts expressed essentially Olig2 (97%), nestin (98%), and Ki67 (71%) while they were negative for OPC markers PDGFRα and O4 or neuronal marker MAP2 in vitro, before engraftment (Mozafari et al., 2015). For in vivo cell tracking, NPCs were transduced with a third-generation lentiviral vector encoding the green fluorescent protein GFP. More than 80% of the cells were labeled with this method (Laterza et al., 2013).

2.1.3 | Human iPSC-OPCs

The methods to generate and maintain the human OPCs from iPSCs were previously described (Ehrlich et al., 2017). Briefly, iPSCs were differentiated into NPCs by treatment with small molecules as described (Ehrlich et al., 2017; Reinhardt et al., 2013). Differentiation of NPCs into O4+ oligodendroglial cells was achieved with a polycistronic lentiviral vector containing the coding regions of the human transcription factors SOX10, OLIG2, and NKX6.2 (SON) followed by an IRES-pac cassette allowing puromycin selection for 16 hr (Ehrlich et al., 2017). Human NPCs were seeded at 1.5×10^5 cells/well in 12-well plates, allowed to attach overnight and transduced with SON lentiviral particles and 5 μg/ml protamine sulfate in fresh NPC medium. After extensive washing, viral medium was replaced with glial induction medium (GIM). GIM was replaced after 4 days with differentiation medium. After 12 days of differentiation, cells were dissociated by accutase treatment for 10 min at 37°C, washed with PBS, resuspended in PBS/0.5% BSA buffer, and singularized cells filtered through a 70 μm cell strainer (BD Falcon). Cells were incubated with mouse IgM anti-O4-APC antibody (Miltenyi Biotech) following the manufacturer's protocol, washed, resuspended in PBS/0.5% BSA buffer (5×10^6 cells/ml), and purified by magnetic cell sorting using anti-O4 MicroBeads (Miltenyi Biotec) following the manufacturer's protocol. Media details were provided in Ehrlich et al. (2017).

In vitro characterization by immunocytochemistry revealed that the human iPSC-OPCs were NG2+ and highly expressed GALC and O4 (70%) after 28 days in vitro (Ehrlich et al., 2017). MACS-purified O4+ cells cultured for 14 days in vitro were used for in vivo studies.

2.2 | Animals

To study the dynamic expression of oligodendrocyte Cx47 following demyelination and remyelination after engraftment, we used two different immunodeficient mouse strains: nude mice with normal myelination and *Shi/Shi:Rag2*$^{-/-}$ with dysmyelination (MBP deficient mice) backgrounds as previously published (Mozafari et al., 2015). *Nude mice* were adult *RJ:NMR-Fonx1nu/Fonx1nu* immunodeficient mice (n = 20, 8–9 weeks of age, Janvier). Shiverer mice were crossed to Rag2 null immunodeficient mice (Shinkai et al., 1992) to generate a line of *Shi/Shi:Rag2*$^{-/-}$ dysmyelinating immunodeficient mice (n = 21, 8–9 weeks of age). Mice were housed under standard conditions of 12-hr light/12 hr dark with ad libitum access to dry food and water cycle at ICM institute's animal facility. Experiments were performed according to European Community regulations and were approved by the National Ethic's Committee (authorization 75-348; April 20, 2005) and local Darwin Ethic's Committee.

2.3 | Demyelination and cell transplantation

To induce demyelination, mice were anaesthetized by intraperitoneal injection of a mixture of 100 mg/kg ketamine (Alcyon) and 10 mg/kg xylazine (Alcyon). Focal demyelination was performed as previously described (Blanchard et al., 2013; Buchet, Garcia, Deboux, Nait-Oumesmar, & Baron-Van Evercooren, 2011; Mozafari et al., 2015) by stereotaxic injection of 1 μl of 1% LPC (Sigma-Aldrich) in 0.9% NaCl

into the dorsal funiculus of the spinal cord at the level of the 13th thoracic vertebrate. Forty-eight hours after demyelination, mice received a single injection (1 μl, 10^5/μl) of GFP+ miPSC-NPCs (n = 6/genotype) or mouse embryonic NPCs (mE-NPCs; n = 6/genotype) or the same amount of medium (n = 6/genotype) at the site of demyelination as previously described (Mozafari et al., 2015). All injections (LPC, medium or cells) were performed at low speed (1 μl/2 min) using a stereotaxic frame equipped with a micromanipulator and a Hamilton syringe. For sacrifice, mice were perfused transcardially with a solution of 1X PBS and 4% paraformaldehyde. Nude mice (n = 18) were sacrificed at 1, 2 week(s) postgrafting (wpg) or medium (wpm) (n = 3 per condition and time point). Two intact nude mice were sacrificed at the age of 8–9 weeks. *Shi/Shi:Rag2*$^{-/-}$ mice were sacrificed (n = 3 per condition and time point) at 6 and 10 wpg, 6 and 10 weeks wpm. Three intact *Shi/Shi:Rag2*$^{-/-}$ mice were sacrificed at the age of 16 weeks. After dissection, tissues were postfixed in the same fixative for 1 hr and then processed in 20% sucrose in 1X PBS overnight. Spinal cords (∼12 mm, including the lesion site at the center) were transversally cut in three to five pieces (∼3 mm each), which were serially ordered in small plastic containers, embedded in cryomatrix (Shandon), frozen in cold isopentane at −60°C and stored at −20°C until use. Serial transverse sections were performed at 12 μm with a cryostat (Leica) and collected on 3 series of 10 slides each (30–50 sections/slide). Our published data showed that the density of the grafted GFP+ cells was similar for both miPSC-NPCs and mE-NPCs at 1 and 2 wpg confirming the reproducibility of the lesion/graft paradigm (Mozafari et al., 2015).

One series of *Shi/Shi:Rag2*$^{-/-}$*mice* (n = 3) was also engrafted with human iPSC-OPC, sacrificed at 12 wpg and handled as above (Ehrlich et al., 2017).

2.4 | Immunohistochemistry

Table S1 summarizes the list of antibodies used in this study. Demyelination was revealed using anti-MOG (mouse IgG1 hybridoma Clone C18C5, 1:50) antibody. Transplanted mouse cells were identified with an antibody directed against GFP (GFP-1020, Aves, chicken, 1:200). Differentiated oligodendrocytes were recognized using anti-CC1 (Millipore, OP80, IgG2b, 1:100) or antihuman NOGOA for grafted human OPC (Santa Cruz Biotechnology, sc-11030, goat, 1:50) antibodies. Oligodendroglial lineage cells were identified using anti-Olig2 (Millipore, AB 9610, rabbit, 1:400). Mouse astrocytes were revealed by and anti-nestin (Millipore, MAB353, IgG1, 1:200) and anti-GFAP (Z0334, Dako, rabbit, 1:500) or by anti-GFAP (PA5-18598, Thermo-Fisher Scientific, 1:200). Human astrocytes were detected using anti human GFAP, STEM123 (Y40420, Takara, IgG1, 1:500).

Exogenous myelin was revealed using anti-MBP (Merck Millipore, AB980, rabbit, 1:100) and neurofilaments were identified using anti-NF200 (N0142, Sigma, IgG1, 1:200). Oligodendrocyte Cx47, and Cx32 were revealed respectively with anti-Cx47 (Invitrogen, 4A11A2, IgG1, 1:200) and with anti-Cx32 (Invitrogen, 5F9A9, IgG2a, 1:200). Astrocyte Cx43 and Cx30 were revealed respectively with anti-Cx43 (Sigma-Aldrich, C6219, rabbit, 1:50) and anti-Cx30 (Invitrogen, 71-2200). For MBP and MOG staining, slices were pretreated with ethanol (10 min at room temperature). For connexin staining, sections were pretreated with methanol (10 min, −20°C). Sections were incubated with the corresponding secondary antibodies from Jackson Immunoresearch Europe, or Alexa-conjugated antibodies (Invitrogen) containing Hoechst dye (1 mg/ml). A Carl Zeiss microscope equipped with ApoTome.2 was used for tissue scanning, cell visualization and imaging.

2.5 | Quantification

2.5.1 | Demyelination and panglial loss extension

The extent of demyelination (area with loss of MOG) and panglial loss (area with loss of Cx47 and Cx43 staining) were evaluated based on the percentage of each related immunoreactivity-depleted area out of the total area of the dorsal funiculus (MOG+) at 1 wpg as previously described (Mozafari et al., 2015). Briefly, for each animal, six coronal serial sections apart of 120 μm, from the middle of the lesion site were quantified for different groups of mice grafted with miPS-NPCs and mE-NPCs or injected with medium (n = 3 per group).

2.5.2 | Mature oligodendrocytes and Cx47 dynamic expression

$CC1^+$ cells (endogenous GFP^- or exogenous GFP+) expressing or not the Cx47 were quantified on transverse sections at the lesion site to determine the total number of $CC1^+$ cells or the proportions of total $CC1^+$ mature oligodendrocytes expressing Cx47. For each animal, six coronal serial sections distant of 120 μm, were collected from the middle of the lesion site. The lesion area was defined by MOG and/or Cx47 depletion. Cell density was identified by Hoechst staining of all cell nuclei on adjacent sections. Sections were first scanned at 20X to define the limits of the lesion and level of maximal demyelination, and magnified at ×40 to quantify the amount of GFP cells expressing Cx47. Cell counts were expressed as the percentage of total $CC1^+$, total $CC1^+/GFP^-$ or total $CC1^+/GFP^+$ cells in the lesion area.

2.5.3 | Cx43 dynamic expression

Due to the diffuse nature of Cx43 immunoreactivity, Cx43 assessment was based on the level of intensity of Cx43 staining in the dorsal funiculus (per mm^2) for each condition and at early time points following demyelination, and at later time points during remyelination.

2.5.4 | Donor-derived remyelination

Exogenous myelin was visualized by MBP staining on transverse sections collected from transplanted *Shi/Shi:Rag2*$^{-/-}$ (6 and 10 wpg) mice. At the lesion core, the percentage of NF^{+}/MBP^{+} axons over total number NF^{+} axons was quantified from three different fields of 1,000 μm^2 each per coronal section (on confocal images) and for three sections apart of 120 μm intervals (total number of nine different fields per animal) for all the grafted *Shi/Shi:Rag2*$^{-/-}$ mice at 6 and 10 wpg as previously described (Mozafari et al., 2015).

2.6 | Statistics

Data were analyzed using two-way analysis of variance followed by Tukey's or Sidak's multiple comparison tests or Mann–Whitney test (for less than two groups). Nonnormally distributed data were analyzed by the corresponding non-parametric tests. Statistical analysis was carried out using GraphPad Prism 8 software. Data were presented as mean ± *SEM* for all statistical analysis. A *p* value of less than .05 was considered significant.

3 | RESULTS

3.1 | Oligodendrocytes are frequently connected to astrocytes via Cx43/Cx47 GJs in the intact spinal cord

We first questioned how adult murine oligodendrocytes and astrocytes anatomically connect to each other in the spinal cord of adult mice. To this aim, intact spinal cords of adult nude mice (at 8 weeks of age) were stained for Cx47 and Cx43, the main oligodendrocyte and astrocyte connexins, respectively. Data show that in the dorsal funiculus, the panglial network consists of CC1^{+} oligodendrocytes expressing Cx47 that were frequently co-labeled with astrocyte Cx43

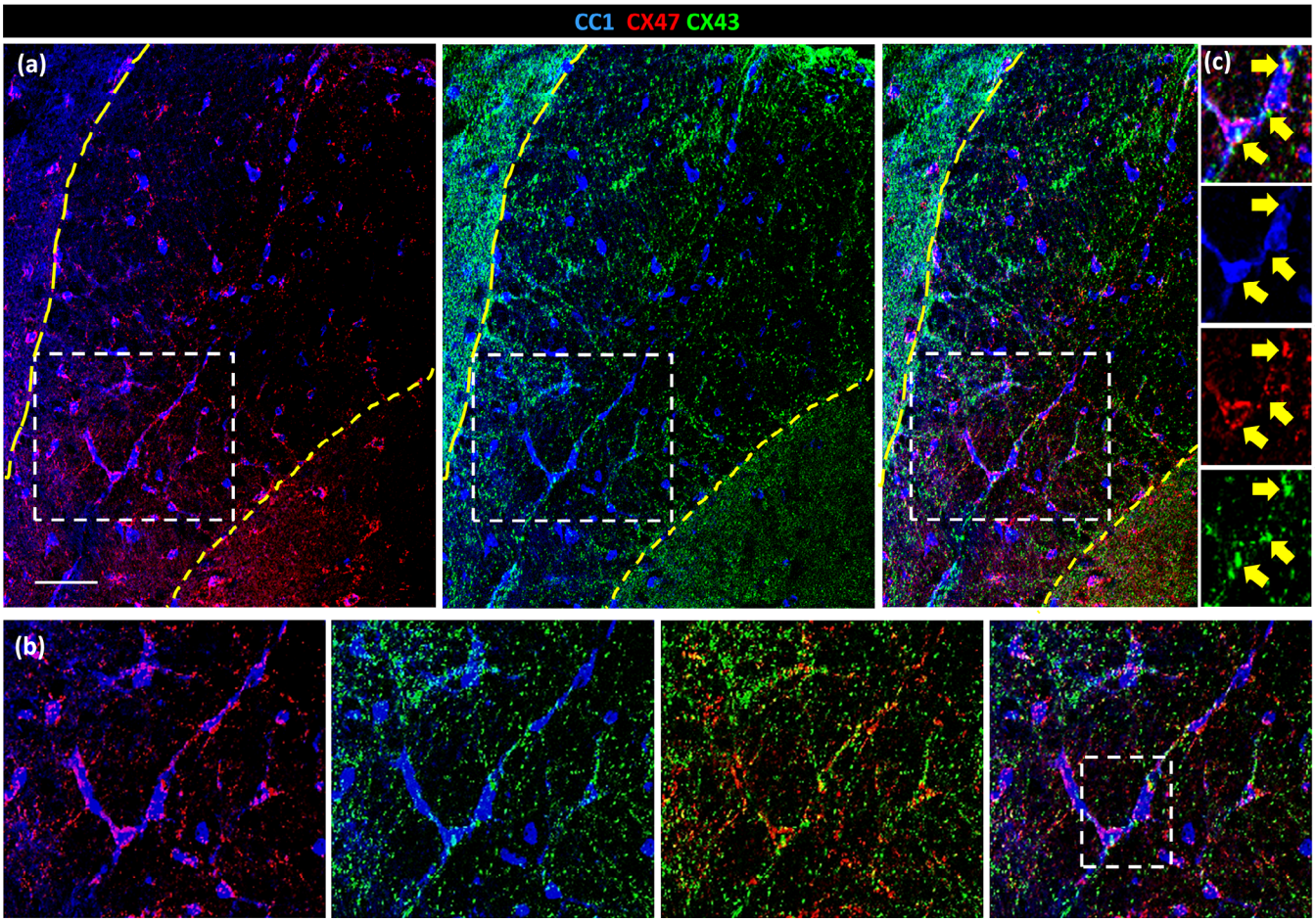

FIGURE 1 Intact panglial network in the spinal cord of adult nude mice. (a) CC1^{+} (blue) oligodendrocytes expressing Cx47 (red) together with astrocyte Cx43 (green) make a network of connected glial cells. (b) Higher magnification of the insets in (a). Dashed yellow lines show the dorsal funiculus. (c) Single channels for the inset in (b) showing two connected oligodendrocytes. Scale bar: 50 μm. See also Figure S1

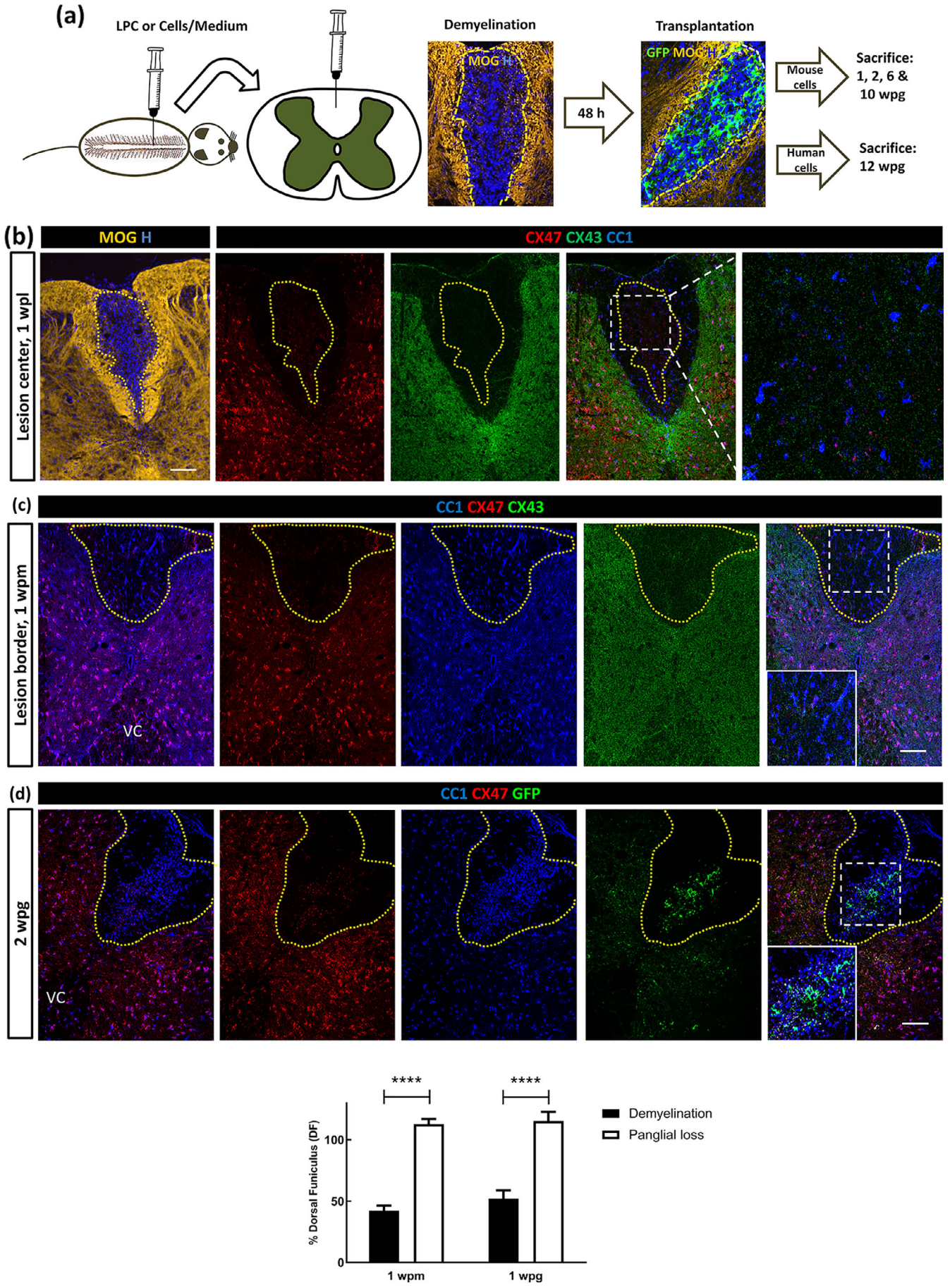

FIGURE 2 Legend on next page.

making a network of glial cells (Figure 1a). Oligodendrocytes were also connected to each other by homologous Cx47/Cx47, which were distributed mainly on their soma (Figure 1b,c). Similar expression was observed on the spinal cord of *Shi/Shi:Rag2*$^{-/-}$ mice at 16 weeks age (Figure S1) indicating that Cx47 and Cx43 expression is maintained in the dysmyelinated mutant.

3.2 | Deconstruction of the panglial network following LPC-induced demyelination overpasses the extent of demyelination

Next, we asked what would be the consequence of demyelination on the existing panglial network and whether grafted NPCs would modulate the impact of demyelination. To answer this question, we took advantage of a simplified focal demyelination model injecting 1 μl LPC (1%) in the dorsal funiculus of the spinal cord of adult *Shi/Shi:Rag2*$^{-/-}$ (myelin-deficient, immune-deficient) or nude (myelin-wild type, immune deficient) mice, (see the study design in Figure 2a), and injected either medium (1 μl), mouse iPSC- or embryonic brain-derived NPCs (100,000 cells in 1 μl) in the lesion, 48 hr after demyelination. The animals were sacrificed 1, 2, 6, and 10 wpg or wpm. Immune deficient animals were used to avoid immune rejection of the transplanted cells and the shiverer-MBP deficient mice were used to visualize the graft derived MBP$^+$ myelin at later stages.

Analysis of the medium injected mice showed that LPC-induced demyelination disrupted the panglial network as evidenced by the lack of expression of Cx47 and the obvious reduction of Cx43 expression 1 wpm (Figure 2b). Evaluation of the demyelinated MOG$^-$ area and Cx47$^-$/Cx43$^-$ area at the lesion center revealed that the panglial network disruption was significantly larger in size than the demyelination area (Figure 2e) with a lack of expression of Cx47 and Cx43 at the lesion border despite the presence of endogenous CC1$^+$ oligodendrocytes, at 1 wpm compared with nondemyelinated ventral column on the same section containing CC1$^+$/Cx47$^+$ cells expressing Cx43, Figure 2c). The panglial loss was also obvious in grafted lesions and was still present at 2 wpg (Figure 2d).

3.3 | Oligodendrocytes gain Cx47 expression as they repopulate the demyelinated lesion

To study the dynamics of loss and gain of Cx47 expression following demyelination, we quantified the number of CC1$^+$/Cx47$^+$ oligodendrocytes at the lesion site in nude mice grafted with either miPSC-NPCs or mE-NPCs or injected with medium 1 and 2 wpg/wpm. Since no difference in Cx47 expression over time was observed between the two grafted cell types (Figure S2), data from the two cell types were pooled and compared with those of medium-injected ones. It is of note that our previous comprehensive study comparing side-by-side the two cell types over time in the same animal model showed no significant difference in terms of initial cell density and subsequent proliferation, migration, and differentiation in oligodendrocytes and myelin-forming cells (Mozafari et al., 2015).

Quantification showed that the total number of mature CC1$^+$ oligodendrocytes, was significantly increased up to the level of intact mice at 2 wpm/wpg as compared to 1 wpm/wpg with no significant difference between graft versus medium injected groups at both time points (Figure 3a–e). While up to 98% of CC1+ oligodendrocytes were expressing Cx47 in intact mice, the percentage of CC1$^+$/Cx47$^+$ over the total CC1$^+$ oligodendrocyte population increased significantly after demyelination, and up to 60% at 2 wpm or 2 wpg (Figure 3f). Almost all of the CC1$^+$/Cx47$^+$ cells were found at the border of the lesion at 2 weeks postdemyelination for both medium and graft injected mice (Figure 3c,d) with no CC1$^+$/C47$^+$ oligodendrocytes at the lesion core at 1 and 2 wpm/wpg (see insets in Figure 3a–d). In the grafted mice, only few GFP$^+$/CC1$^+$/Cx47$^+$ cells were found with small amounts of Cx47 expression, and no significant increase at 2 versus 1 wpg (Figure 3g).

Next, we asked whether the grafted cells had any impact on the percentage of endogenous oligodendrocyte expressing Cx47. The percentage of GFP$^-$/CC1$^+$/Cx47$^+$ over total CC1$^+$ cells increased significantly in the grafted mice at 1 and 2 wpg (Figure 3g) suggesting that the grafted cells induced Cx47 expression by endogenous oligodendrocytes. Interestingly, some CC1+ cells slightly co-labeled with astrocyte Cx43 at 1 wpg and their number increased slightly at 2 wpg (insets in Figure 3a–d). GFP$^+$/Cx43$^+$ cells were the source of many of these Cx43$^+$ plaques at 1 or 2 wpg consistent with the observation

FIGURE 2 Demyelination disrupts the panglial network beyond the demyelinating zone. (a) Experimental design. Demyelination is induced by lysolecithin (LPC) injection in the dorsal funiculus (DF) of adult nude or *Shi/Shi:Rag2*$^{-/-}$ mice. Mouse induced pluripotent stem cell (iPSC)-derived neural precursors (NPCs), mouse embryonic NPCs, or medium were injected 48 hr after demyelination and animals sacrificed 1 and 2 wpg/wpm for nude mice and 6 or 10 wpg/wpm for *Shi/Shi:Rag2*$^{-/-}$ mice. A group of *Shi/Shi:Rag2*$^{-/-}$ mice were grafted with human iPSC- OPCs and sacrificed 12 wpg. (b) Depletion of MOG staining (yellow) shows a defined area of LPC-induced demyelination 1 week postinjection. The loss of Cx47 (red) or Cx43 (green) expression by the CC1$^+$ oligodendrocytes (blue) extends beyond the lesion limits. (c) Although CC1$^+$ cells (blue) are present at the lesion border, expression of oligodendrocyte Cx47 (red) and astrocyte Cx43 (green) is lost compared to the ventral column (VC) where many CC1$^+$/Cx47$^+$ or Cx43$^+$ cells are present. (d) The panglial loss following LPC-induced demyelination is still present in a large area around the lesion 2 wpg. (e) Quantification shows that in both medium and cell injected dorsal funiculus, the panglial loss area (dashed yellow line in (c) and (d)) is significantly larger in size than the lesion area (dashed yellow line in (b)). Two-way analysis of variance (ANOVA) followed by Tukey's multiple comparison tests were used for the statistical analysis of these experiments (n = 3–6 mice per group). Error bars represent *SEM*s. ****p < .0001. Scale bars: 100 μm

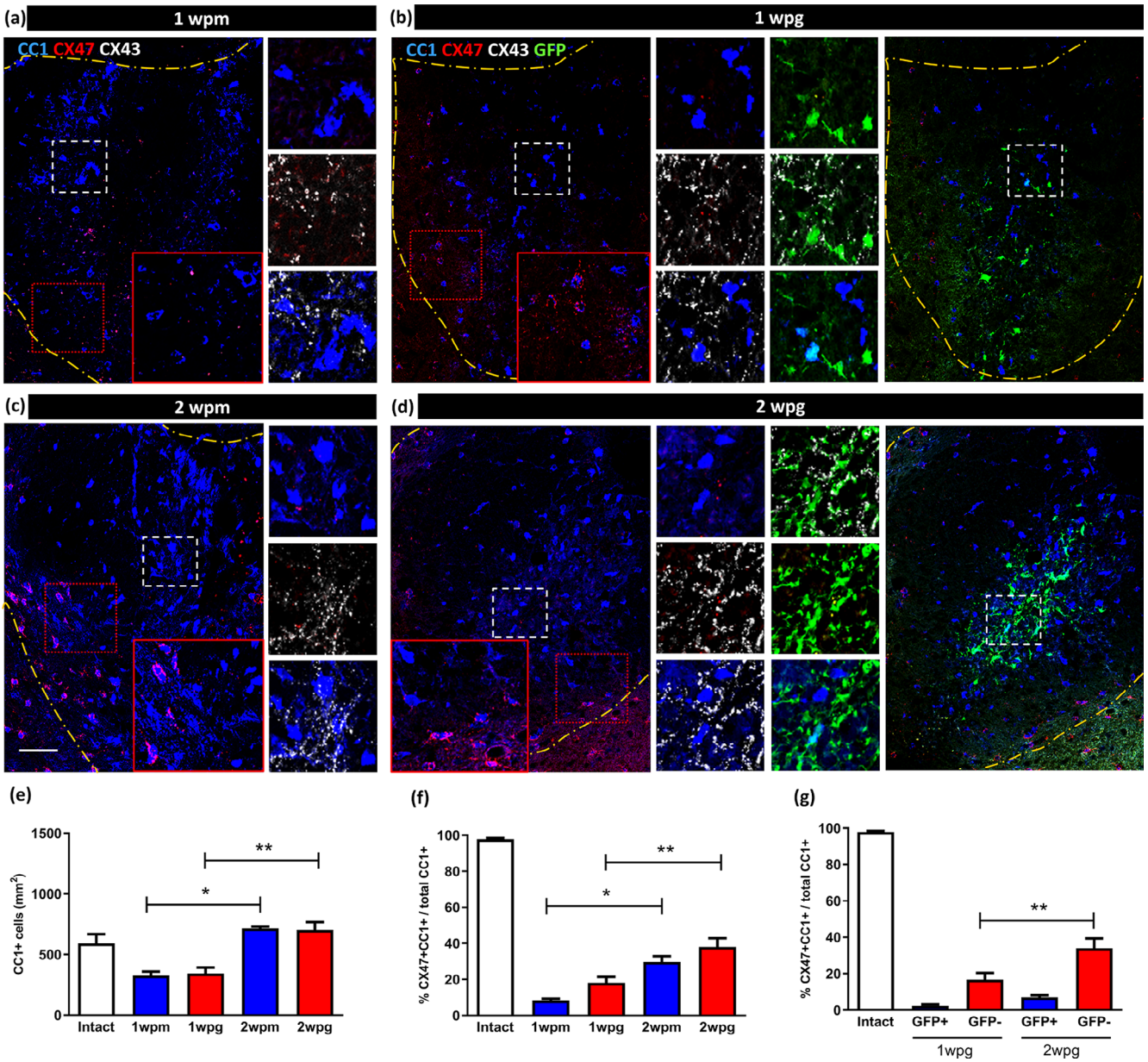

FIGURE 3 Dynamics of oligodendrocyte Cx47 loss and gain of expression by endogenous and exogenous cells following demyelination. (a,b) In 1 wpm/wpg nude mice spinal cords, the number of $CC1^+$ cells (blue) was decreased, and both endogenous or grafted GFP^+ cells (green) were almost entirely negative for the oligodendrocyte-specific Cx47 marker (red) at the center of the lesion (inset boxes with dashed white lines). (c,d) Few oligodendrocytes co-expressed the astrocyte specific Cx43 marker (white). (e) The number of $CC1^+$ cells increased significantly 2 wpm or wpg with a slight increase in $CC1^+/Cx47^+$ found mainly at the border of the dorsal funiculus (red inset boxes) as compared to the 1 wpm/wpg. (f) Quantification indicates that the percentage of $Cx47^+/CC1^+$ cells was significantly increased at 2 wpm/wpg. (g) In the grafted animals, the percentage of $GFP^+/Cx47^+$ oligodendrocytes did not increase significantly over time, while the percentage of $Cx47^+/GFP^-$ endogenous oligodendrocytes did. Dashed yellow lines show the limits of dorsal funiculus in (a–d). One-way analysis of variance (ANOVA) followed by Tukey's multiple comparison tests were used for the statistical analysis of these experiments (n = 3–6 mice per group). Error bars represent *SEM*s. *p < .05, **p < .001. wpg: week(s) postgraft; wpm: week(s) postmedium; scale bar: 50 μm

that many GFP^+ were $GFAP^+$/$nestin^+$ around the lesion at 1 wpg (Figure S3).

Further quantification revealed a tendency of decrease in the level of astrocyte Cx43 expression at 1 wpm as compared to 2 wpm, 1 and 2 wpg (Figures 4a–d and S4c).

3.4 | Gain of Cx47 expression during remyelination is accelerated by exogenous NPCs

We previously demonstrated that miPSC-derived NPCs competitively remyelinated numerous demyelinated host axons with compact

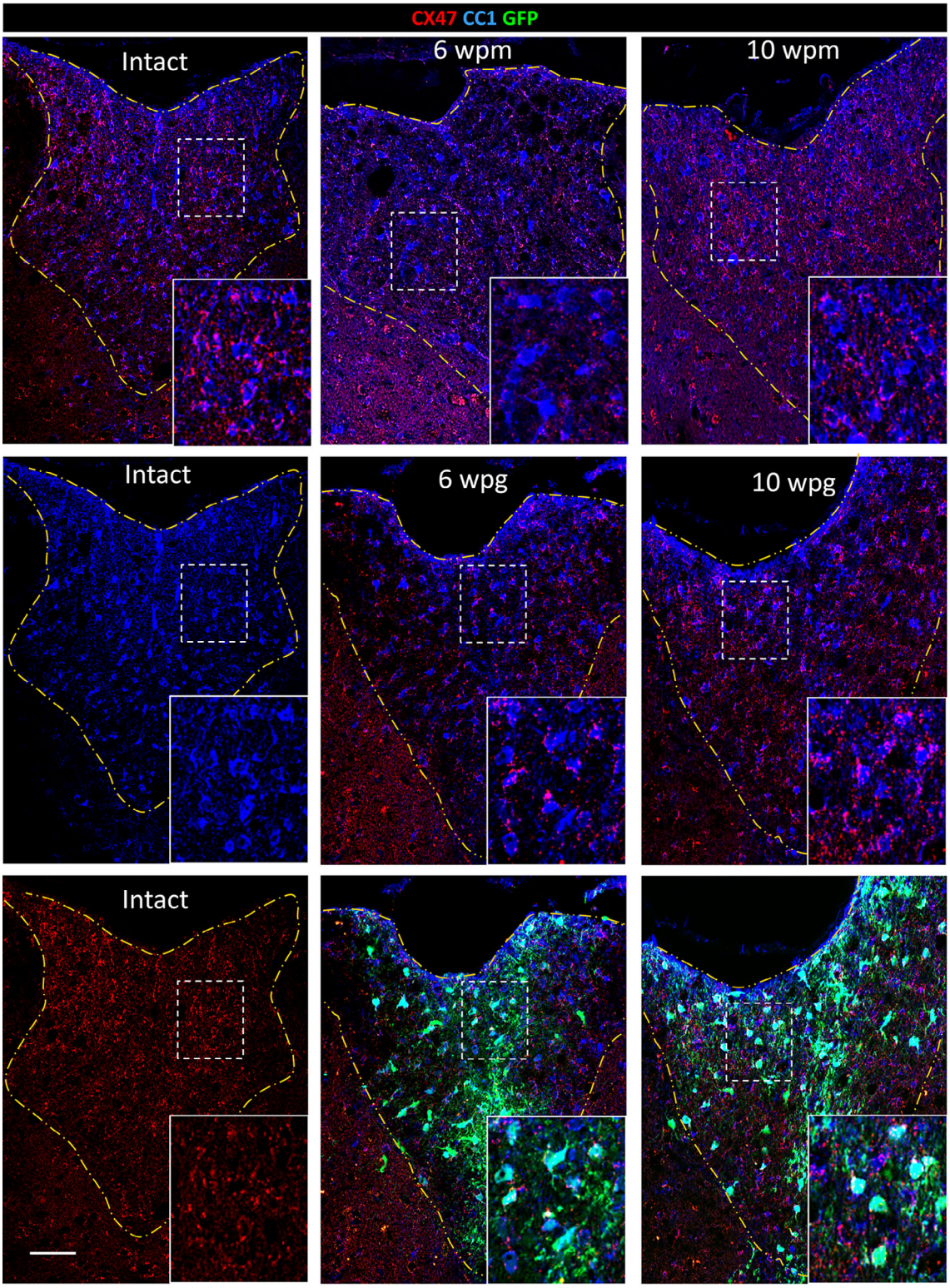

FIGURE 4 Dynamics of oligodendrocyte Cx47 gain of expression during endogenous and exogenous remyelination. Expression of Cx47 (red) by $CC1^+$ oligodendrocytes (blue) after medium or engraftment of miPSC-neural precursors (NPCs) in the *Shi/Shi:Rag2*$^{-/-}$ dorsal funiculus (dashed yellow lines) was compared to intact mice. At 6 wpg, $CC1^+$ cells expressed more $Cx47^+$ plaques compared to 6 wpm. Yet, there was no difference with intact and 10 wpm mice. At 10 wpg, $CC1^+$ oligodendrocytes expressed more $Cx47^+$ plaques compared to 6 wpg, 10 wpm and intact mice. Scale bar: 50 μm. wpg: week(s) postgraft; wpm: week(s) postmedium; quantitative data are reported in Figure 5

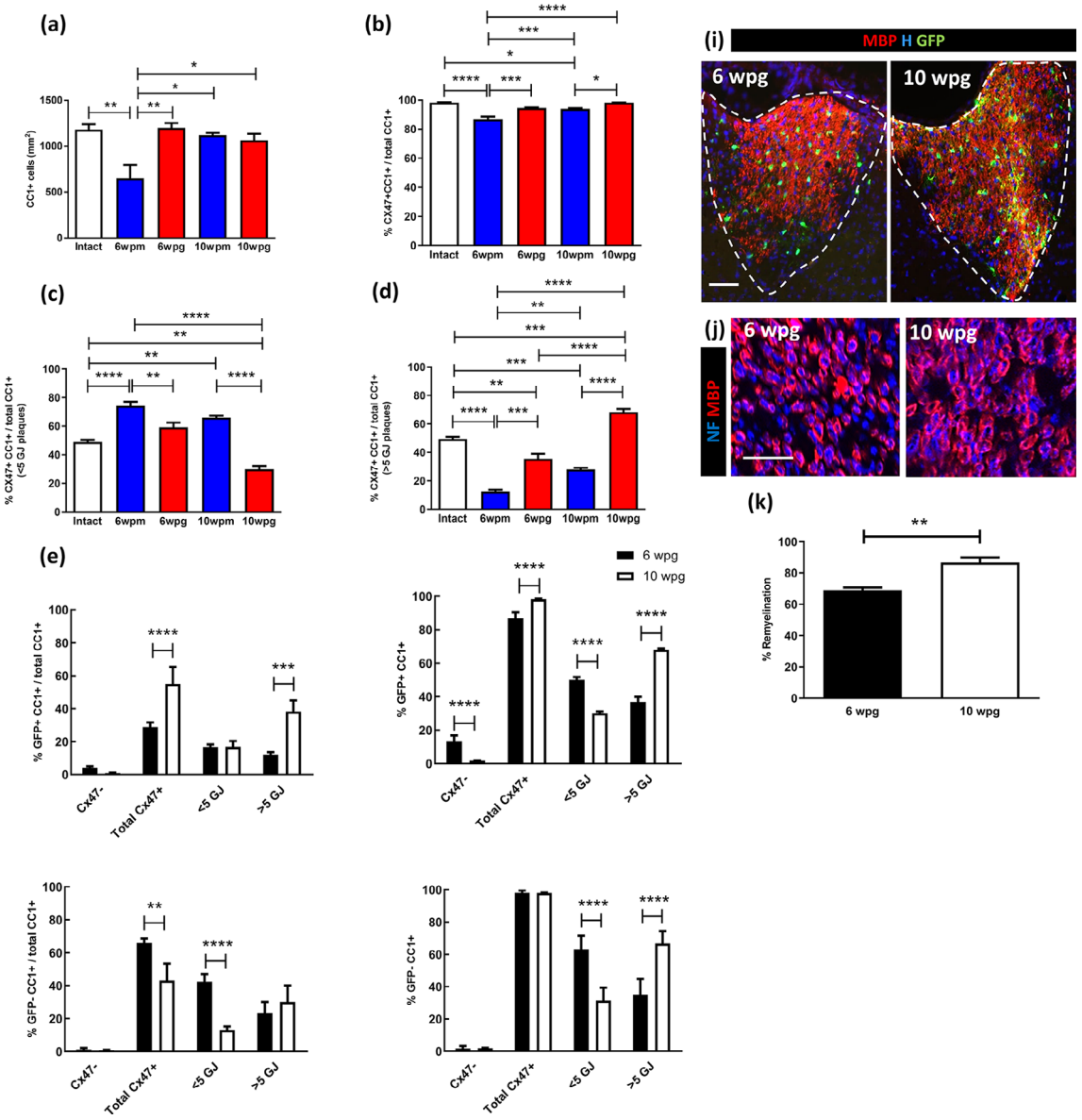

FIGURE 5 The dynamic expression of Cx47 following demyelination, is accelerated by grafted neural precursors (NPCs). (a) The total number of $CC1^+$ cells in the lesion was significantly lower at 6 wpm as compared to intact, 6 wpg, 10 wpm, and 10 wpg mice. (b) The total number of $CC1^+$ cells did not increase after engraftment. The decrease in $CC1^+/Cx47^+$ cells in 6 wpm mice over intact mice was rescued in 6 wpg mice. While at 10 wpm, the percentage of $CC1^+/Cx47^+$ cells was not fully recovered to that of intact mice, it was fully rescued in 10 wpg mice. No significant difference was observed in the percentage of $CC1^+/Cx47^+$ cells between 6 and 10 wpg (see Figure 4). (c) The percentage of $CC1^+/Cx47^{low}$ cells in 6 and 10 wpm mice was significantly higher than that in intact mice. $CC1^+$ oligodendrocytes expressed lower amounts of Cx47 plaques respectively at 6 and 10 wpg as compared to 6 and 10 wpm. (d) In 10 wpg mice, the percentage of $CC1^+/Cx47^{low}$ cells was significantly lower than that of intact mice. The percentage of $CC1^+/Cx47^{high}$ was significantly lower in 6 wpm, 10 wpm, and 6 wpg compared to intact mice, but rescued over intact mice at 10 wpg. (e) Grafted cells constituted more than 50% of total $CC1^+/Cx47^+$ cells at 10 wpg with most of them expressing high levels of Cx47 plaques. (f) Cx47 expression by the $GFP^+/CC1^+$ population increased significantly over time with higher Cx47 expression at 10 wpg versus 6 wpg. (g) In the grafted mice, endogenous $CC1^+/Cx47^+$ cells constitute a higher proportion of total CC1+ cells (most of them were $CC1^+/Cx47^{low}$ cells) at 6 wpg but decreased over time (compare (g) to (e)). (h) In the grafted mice, almost 100% of the endogenous $CC1^+$ cells expressed Cx47 at 6 wpg as well as 10 wpg and gained more Cx47 plaques over time (see Figure 4). (i) Remyelination (MBP expression in red) of the grafted cells (green) in dorsal funiculus increased over time. (j,k) The percentage of NF^+ host axons (blue) enwrapped with exogenous MBP^+ myelin increased significantly over time. One-way followed by Tukey's (graphs in (a–d)), two-way analysis of variance (ANOVA) followed by Sidak's multiple comparison tests (graphs in (f–h)) or Mann–Whitney test (graph in (k)) were used for the statistical analysis of these experiments (n = 3 mice per group). Error bars represent *SEMs*. *p < .05, **p < .001, *** or ****p < .0001. wpg: week(s) postgraft; wpm: week(s) postmedium. Scale bars: 50 μm (in (i)) and 10 μm (in (j))

myelin, restored nodes of Ranvier and rescued the delayed conductance velocity of *Shi/Shi Rag2*$^{-/-}$ mice to the same extent than brain-NPCs (Mozafari et al., 2015). Here, we aimed to study in the same context, the effect of the graft on the temporal dynamics of Cx47 expression during the remyelination process. To this end, we quantified the number of the CC1^{+}/Cx47^{+} cells in the intact, grafted, and medium injected control mice, at 6 and 10 weeks after spinal cord demyelination (Figure 4).

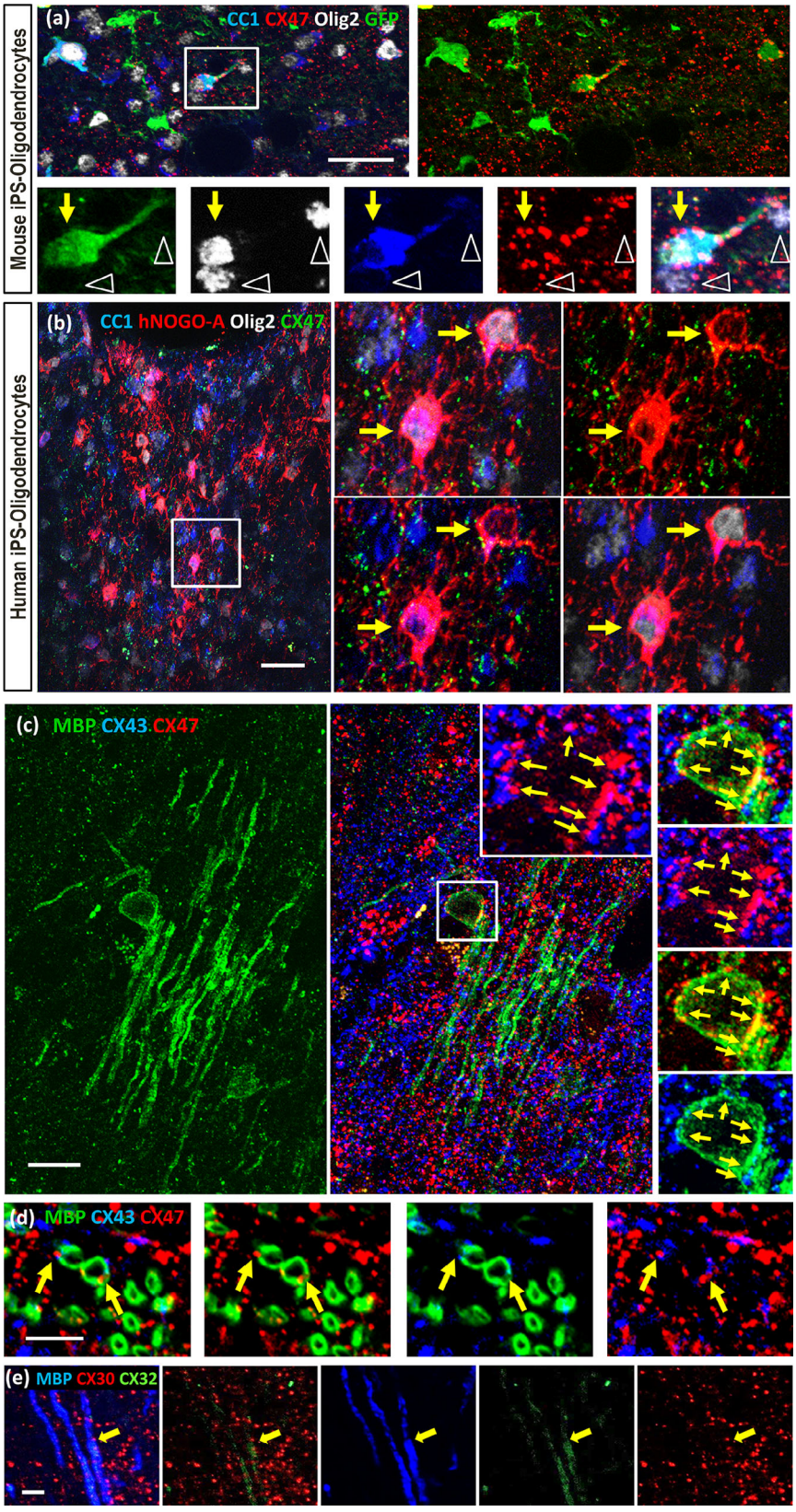

FIGURE 6 Induced pluripotent stem cell (iPSC)-derived oligodendrocytes have the molecular machinery to interact with other glial cells. (a) Mouse GFP^{+} (green)/CC1^{+} (blue)/Olig2 + (gray) iPSC-derived oligodendrocyte expressing Cx47 (red). (b) Human iPSC-derived CC1^{+} (blue)/Olig2^{+} (gray)/hNOGOA^{+} (red) oligodendroglia expressing Cx47 (green) integrated into the demyelinated dorsal funiculus. (c) A mouse iPSC-derived oligodendrocyte expressing MBP^{+} myelin (green) connected to astrocytes via heterologous gap junctions (GJs) Cx47/Cx43 (red:blue) on their soma (inset, yellow arrows). (d) Graft-derived MBP^{+} myelin-like structures seen in cross sections (green) decorated by Cx47^{+} plaques (red). (e) Oligodendrocyte Cx32 was also found in conjunction with its astrocyte counterpart Cx30 on IPS-derived MBP+ myelin (e). Scale bars: 50 μm (in (a) and (b)), 25 μm (in (c)), and 5 μm (in (d) and (e))

In the medium group, the total number of $CC1^+$ cells was reduced at 6 wpm as compared to intact mice but was rescued at 10 wpm (Figure 5a). The total number of $CC1^+$ cells did not increase after engraftment (Figure 5a). As for the percentage of $CC1^+/Cx47^+$ cells (Figure 5b), it was significantly lower at 6 wpm as compared with intact mice but was partially restored at 10 wpm to levels of intact mice. In contrast, the percentage of $CC1^+/Cx47^+$ cells in the transplanted group remained steady at 6 wpg, and 10 wpg, and was comparable to the levels of intact mice. Figure 4 showed that the amount of $Cx47^+$ GJ varies among the intact, medium, and grafted mice. To gain insight in the differences in oligodendrocyte Cx47 expression levels per group, we quantified the number of Cx47 plaque expression per $CC1^+$ cells and namely CC1+ cells with 5 or less (≤ 5, $Cx47^{low}$), and those with more than 5 (>5, $Cx47^{high}$) Cx47 plaques. In the intact *Shi/Shi:Rag2*$^{-/-}$ mice, nearly 48% of $CC1^+$ cells were $Cx47^{low}$ and 49% were $Cx47^{high}$ (Figure 5c,d). The percentage of $CC1^+/Cx47^{low}$ cells was significantly higher in the medium group at 6 wpm (74%) as compared to the intact, and grafted groups at 6 wpg and 10 wpg. At 10 wpm, the percentage of $CC1^+/Cx47^{low}$ cells (Figure 5c) was significantly higher (65%) than that in the intact and 10 wpg mice. The $CC1^{+/}Cx47^{low}$ population represented 59 and 29% of total $CC1^+$ cells respectively at 6 and 10 wpg. The percentage of $CC1^+/Cx47^{high}$ cells (Figure 5d) increased significantly over time for both medium-treated and grafted mice (from 12% at 6 wpm to 28% at 10 wpm, and 35% at 6 wpg to 68% at 10 wpg). Interestingly the higher percentage of $CC1^+/Cx47^{high}$ cells in the grafted group at 10 wpg was significantly higher than that of intact mice. These data suggest that during remyelination, Cx47 expression levels in grafted mice were not only accelerated compared to medium-treated mice, but also exceeded that of intact mice.

Next, we questioned the relative contributions of grafted (GFP+) and endogenous (GFP–) oligodendrocytes to the Cx47 expression in grafted mice (Figure 5e,g). Data show that the $GFP^+/CC1^+/Cx47^+$ oligodendrocytes consist of 28 and 55% of total $CC1^+$ cells respectively at 6 and 10 wpg. In addition, at 10 wpg, the $GFP^+/ CC1^+/Cx47^{high}$ pool contributed majorly (38%) to the $GFP^+/CC1^+/Cx47^+$ increase (Figure 5e). In addition, the percentage of $Cx47^+$ cells as well as Cx47 level of expression increased over time in the grafted oligodendrocyte population, (Figure 5f) with 86% and 98% of $GFP^+/CC1^+$ cells expressing Cx47, respectively, at 6 wpg (50% $Cx47^{low}$ and 36% $Cx47^{high}$) and 10 wpg (30% $Cx47^{low}$ and 68% $Cx47^{high}$).

How transplanted cells impact on endogenous $Cx47^+$ oligodendrocytes was our next question. Quantification showed that in the transplanted shiverer mice, endogenous $GFP^-/CC1^+/Cx47^+$ cells constitute 66% of the total $CC1^+$ population with 42% $Cx47^{low}$ at 6 wpg (Figure 5g). As the percentage of $GFP^+/CC1^+/Cx47^+$ cells increased to 55% at 10 wpg, the percentage of endogenous $GFP^-/CC1^+/Cx47^+$ cells decreased to 43% taking into account that the total number of CC1+ cells does not fluctuate in the grafted mice. However, 98% of the endogenous population expressed Cx47 with 63% $Cx47^{low}$ cells and 66% $Cx47^{high}$, respectively, 6 and 10 wpg (Figure 5h).

These data altogether show that during lesion repair, the number of $Cx47^+$ plaques per $CC1^+$ cells increases with time within the total $CC1^+$ population including the endogenous or exogenous GFP^+ oligodendrocyte population.

We then asked whether this increase could be correlated to the progress of remyelination itself. Immunolabeling for MBP and NF revealed that 69% of the axons in the lesion core were remyelinated by the grafted cells at 6 wpg. The proportion of remyelinated axons increased significantly from 68% at 6 wpg up to 86% at 10 wpg (Figure 5i–k). Comparing graphs of Figure 5f with Figure 5k shows that the increase in the number of $Cx47^+$ oligodendrocytes and in the level of Cx47 expression per cell, fluctuates with the progressive increase in remyelination, suggesting that Cx47 expression and remyelination are temporally correlated.

Quantification of Cx43 expression in the dorsal funiculus shows a tendency to increase in the grafted mice both at 6 and 10 wpg (Figure S4a,b,d), although the changes were not statistically significant.

3.5 | The iPSC-derived neural progeny integrates in the panglial network after transplantation in dysmyelinated mice

Imaging at high magnification confirms that mature $CC1^+/Olig2^+$ host- and grafted mouse iPSC-oligodendrocytes were able to express Cx47 during remyelination (Figure 6a). We also observed that not only mature $CC1^+$ oligodendrocytes but also $CC1^-/Olig2^+$ OPCs (empty white arrowheads insets in Figure 6a) express Cx47 and make homologous GJ Cx47/CX47 with adjacent oligodendrocytes (Figure 6a insets).

To investigate whether human iPSC-derived oligodendrocytes were able to express Cx47 in response to demyelination, human iPSC-derived $O4^+$ cells (hiOL) were also grafted in the demyelinated adult *Shi/Shi:Rag2*$^{-/-}$spinal cords(see Figure 2a), and animals sacrificed 12 wpg. In these conditions, hiOL vastly remyelinate the demyelinated spinal cord (Ehrlich et al., 2017). Here, we show that the human iPSC-derived oligodendrocytes identified by CC1, human NOGOA and Olig2 expressed also Cx47 (Figure 6b). Moreover, the iPSC-derived oligodendrocytes were frequently co-labeled with astrocyte Cx43 to make $Cx47^+/Cx43^+$ heterologous GJs (Figure 6c). $Cx47^+/Cx43^+$ co-labeling was found not only on iPSC-oligodendrocyte somas but also on iPSC-derived myelin (Figure 6d). Further integration of iPSC-derived myelin was confirmed by co-labeling of oligodendrocyte Cx32 and its astrocyte counterpart Cx30 on MBP+ fibers (Figure 6e). Our data also confirm that not only host astrocytes (Figure S5a) but also exogenous mouse (Figure S5b) and human (Figure S5c) iPSC-derived astrocytes express Cx43 or Cx30 (Figure S5d). Human GFAP+ astrocytes expressing Cx30 were found in contact with MBP+ myelin (Figure S5e) indicating that grafted iPSC-glia can also make connections between each other. These data suggest that rodent and human iPSC-derived oligodendrocytes and astrocytes have the molecular machinery to interact with other glial cells during remyelination and participate in reconstructing the panglial network lost to demyelination.

4 | DISCUSSION

Alterations in connexin expression by oligodendrocytes or associated astrocytes suggest that GJ components that connect one cell to another play a major role in genetic or acquired myelin disorders (Cotrina & Nedergaard, 2012; Xia et al., 2020). While most myelin disease related studies focused on how to increase re/myelination via axo-glia interactions as a mean to protect and insure axon's proper function, less is known about the panglial syncytium reconstruction in order to provide maintenance of the newly generated myelin and thereby secure full repair of the lesion. We have used LPC-induced demyelination to investigate in detail the dynamic expression of oligodendrocyte Cx47 and astrocyte Cx43 during the demyelination-remyelination process of the adult murine spinal cord. Moreover, we grafted iPSC-NPCs/OPCs following LPC-induced demyelination to explore whether they play a role in the loss and reconstruction of the glial-glial network.

We show that in the intact adult spinal cord of myelin-wild type nude mice, oligodendrocytes express Cx47 and connect to one another, as well as to astrocytes via Cx47 and Cx43 expression as previously reported in the intact mouse corpus callosum (Maglione et al., 2010). LPC-induced focal demyelination alters the panglial network and more specifically disrupts Cx47/Cx47 and Cx47/Cx43 connections. Interestingly, this loss extends beyond the extent of demyelination suggesting that the white matter panglial network is highly sensitive to demyelination, and that a given area of myelin is supported by a larger area of glial-glial connections. This is in line with observations arising from chronic MS lesions both in white and gray matter as well as in normal appearing white matter (NAWM) (Markoullis, Sargiannidou, Schiza, et al., 2012; Markoullis et al., 2014). In MS, connexin loss is correlated with inflammation and disease duration, suggesting that oligodendrocyte disconnection from reactive astrocytes may play a role in failed remyelination and disease progression (Markoullis, Sargiannidou, Schiza, et al., 2012). The confirmation of these observations in the MS animal model, EAE, suggests that GJ deficient myelinated fibers appear more vulnerable to CNS inflammatory demyelination. They also suggest that persistent impairment of both intracellular and intercellular oligodendrocyte GJs even in NAWM may be an important mechanism of MS progression (Markoullis, Sargiannidou, Gardner, et al., 2012). Here, we used the myelin detergent LPC to mimic focal demyelination. Whether the LPC is inducing the loss of Cx43/Cx47, and demyelination is the result or disruption of panglial network is secondary to demyelination needs to be investigated by, for example, inducing LPC lesion in Cx47 or Cx43 overexpressing mice. Nevertheless, the present data imply that LPC-induced focal demyelination might provide a valuable simplified model to study adult panglial loss as observed in demyelinating disorders.

Our data revealed that 2 weeks following demyelination, only few oligodendrocytes around the lesion start to re-express Cx47 despite the increasing number of oligodendrocytes at the lesion site. Down and upregulation of Cx47 occur also in cuprizone-induced demyelination (Parenti et al., 2010) and EAE (Markoullis, Sargiannidou, Gardner, et al., 2012). In the later, Cx47 expression increased during remyelination at 28 dpi but decreased again at 50 dpi in the relapsing phase (Markoullis, Sargiannidou, Gardner, et al., 2012). These observations indicate that connexin expression is a very sensitive and dynamic process occurring in response to any type of demyelination.

We also provide evidence that, engraftment of mouse embryonic or iPSC-derived NPCs results in a higher percentage of endogenous oligodendrocytes expressing Cx47. Interestingly, one study revealed that intraventricular transplantation of NPCs 7 days following EAE induction prevents the reduction of oligodendrocyte Cx47, and increased the number of oligodendrocytes, local Cx47 levels and Cx47 plaques per cell suggesting a neuroprotective role of the transplanted NPCs on the panglial network (Theotokis et al., 2015). How exogenous NPCs induce Cx47 expression in endogenous oligodendrocytes is not known. Yet, an increasing body of evidences support that NPC's neuroprotective effect on endogenous cells occurs via cytokines and/or neurotrophic factors (Laterza et al., 2013; Marteyn et al., 2016; Ottoboni et al., 2020; Pluchino et al., 2020). Moreover, we show that the grafted cells differentiate into oligodendrocytes as well as into GFAP+/Cx43+ astrocytes, which in turn, could help promoting Cx47 expression in endogenous oligodendrocytes (May, Tress, Seifert, & Willecke, 2013). NPCs grafted into a cerebellar organotypic slice culture system have a neuroprotective effect on host neurons through the GJ they make with neurons particularly mediated by astrocytic Cx43 (Jaderstad et al., 2010). In addition, ciliary neurotrophic factor activates the JAK/STAT pathway leading to enhanced Cx43 expression and intercellular coupling (Ozog et al., 2004). Whether Cx47 (or its major partner Cx43) can be upregulated by trophic factors secreted from NPCs needs to be investigated. Moreover, our study shows that the level of Cx43 expression tends to be higher in all the grafted animals both at early time points following demyelination and later time points during remyelination and this could induce Cx47 expression (May et al., 2013) in the endogenous cells.

We found that the percentage of oligodendrocytes expressing Cx47 is accelerated in the grafted animals 6 and 10 wpg compared to medium-injected groups. Moreover, the percentage of oligodendrocytes expressing higher levels of Cx47 increases significantly over time in the grafted animals. Endogenous oligodendrocytes constitute a higher percentage of Cx47+ cells with most of them expressing low levels of Cx47 plaques at 6 wpg. However, at 10 wpg, grafted cells harbor a greater proportion of the total Cx47+ oligodendrocyte population, with most of them expressing high levels of Cx47 plaques, thus suggesting a higher contribution of graft-derived oligodendrocytes in total Cx47 expression over time. Moreover, the percentage of endogenous oligodendrocytes with high levels of Cx47 is clearly higher in the grafted versus medium groups (28% at 10 wpm vs. 66% at 10 wpg) indicating, once more, the beneficial effect of grafted cells on the endogenous cells. In this context, future studies using loss of function experiments in which expression of Cx47 in the grafted cells is blocked should provide valuable information.

We previously demonstrated that mouse or human iPSC-derived NPCs or OPCs grafted in the *Shi/Shi:Rag2*$^{-/-}$ demyelinated spinal cord, extensively remyelinate the lesion (Ehrlich et al., 2017; Mozafari

et al., 2015). Here, we show that the progressive increase in oligodendrocyte Cx47 expression is timely correlated with the increase in remyelination by the grafted cells. These data altogether, suggest that the more oligodendrocytes produce myelin around axons the more they express Cx47 plaques, highlighting the need of remyelinating cells to firmly integrate into the glial network to receive the necessary metabolic/homeostatic support. Inducing demyelination in conditional Cx47 null mice could resolve whether panglial reconstruction or Cx47 restoration follows, facilitates or is concomitant of remyelination.

We also show that grafted cells express oligodendrocyte Cx47, which frequently co-labels with astrocyte Cx43 during remyelination. The observation that exogenous and endogenous oligodendrocytes co-express oligodendrocyte Cx47 and astrocyte Cx43 is in line with the fact that NPC engraftment leads to the reactivation of endogenous astrocytes as well as the differentiation of a small population of the grafted cells into astrocytes. This indicates that both endogenous and exogenous astrocytes could contribute to the astrocyte Cx43 expression on oligodendrocyte somas. Thus, mouse and human skin-derived remyelinating oligodendrocytes are capable of being integrated into the panglial network by establishing proper molecular connections with other glial cells to ensure their functionality. A recent dye-coupling study of human iPSC-derived oligodendrocytes grafted in the corpus callosum of newborn shiverer mice showed that the cells were capable of forming functional GJs with neighbor murine or human glial cells, indicating that exogenous cells could not only myelinate host axons, but also functionally integrate into the host pan-glial network (Mozafari et al., 2020). Although not tested here, it is assumed that exogenous cells also proceed to functional integration into the host pan-glial network during repair.

It is known that Cx43/Cx47 co-expression enables astrocytes to fuel oligodendrocytes the necessary energy supply through GJ-mediated communication (Giaume, Leybaert, Naus, & Saez, 2013; Hirrlinger & Nave, 2014). The use of a mutated form of Cx43, which is only delivered to the plasma membrane, but does not form functional channels, showed that the presence of Cx43 at the cell surface, is necessary and sufficient for normal expression, phosphorylation and stability of Cx47-mediated plaques at the cell surface (independent of Cx43 GJC function on the cell surface), suggesting a dependency of oligodendrocyte Cx47 GJ channel stability on astrocyte Cx43 expression (May et al., 2013).

Although our data clearly support the dynamic expression of Cx47 together with Cx43 during the demyelination-remyelination process, many open questions remain to be answered. These include the mechanism involved in the endogenous-exogenous interface during remyelination, which could lead to the means to pharmacologically accelerate panglial repair following demyelination, the capacity of the panglial network to help support myelin in repeated episodes of dem/remyelination, the functionality of the established connections and finally the respective roles of astrocyte or oligodendrocyte connexins in lesion expansion, and OPCs differentiation and remyelination in order to better clarify the functional consequences of these networks.

Altogether, the data of the present study provide valuable findings in the biology and dynamics of oligodendrocyte Cx47 expression during adult demyelination and remyelination. More specifically, we show that grafted NPCs might help improving remyelination of the lesion, but also participate in- and accelerate reconstruction of the panglial network to ensure their functional integration and the maintenance of the newly generated myelin. This study along with others, indicate that connexin-mediated communication among oligodendrocytes, among astrocytes, and/or between astrocytes and oligodendrocytes may be important for oligodendrocyte development during re/myelination. Despite the lack of definite evidence for the role of GJs in the pathology of adult demyelinating diseases such as MS, these findings shed light on the mechanisms involved in myelin pathology and repair in vivo and imply the role of GJs as contributors or modifying factors during MS pathogenesis or therapy. Deciphering the factors involved in Cx-mediated regulation of oligodendrocyte differentiation or remyelination may provide clues for novel strategies to rescue hereditary dysmyelinating diseases and improve remyelination by manipulating connexin expression or enhancing GJ channel function in acquired demyelinating diseases.

ACKNOWLEDGMENTS

This work was supported by the Progressive MS Alliance (PMSA) Collaborative Research Network PA-1604-08492 (BRAVEinMS) to G. M., A. B. V. E., and T. K.; the National MS Society (NMSS RG-1801-30020) to T. K. and A. B. V. E.; INSERM and ICM Internal Fundings to A. B. V. E.; the Italian Multiple Sclerosis Foundation (FISM), Project "Neural Stem Cells in MS" to G. M. S. M. was funded by the European Committee for Treatment and Research in Multiple Sclerosis (ECTRIMS). A. B. V. E. and S. M. thank the ICM imaging and rodent facilities.

CONFLICT OF INTEREST

The authors declare no conflict of interest.

AUTHOR CONTRIBUTIONS

Sabah Mozafari and **Anne Baron-Van Evercooren**: Conceptualization. **Sabah Mozafari**, **Cyrille Deboux**, **Cecilia Laterza**, **Marc Ehrlich**, **Tanja Kuhlmann**, **Gianvito Martino**, and **Anne Baron-Van Evercooren**: Methodology. **Sabah Mozafari** and **Anne Baron-Van Evercooren**: Formal analysis. **Sabah Mozafari** and **Anne Baron-Van Evercooren**: Writing with editing and discussion from all coauthors. **Sabah Mozafari**, **Anne Baron-Van Evercooren**, and **Gianvito Martino**: Funding acquisition. **Sabah Mozafari** and **Anne Baron-Van Evercooren**: Supervision.

DATA AVAILABILITY STATEMENT

The authors declare that the findings of this study are available in the article and in the supplementary material of this article. The data are available upon reasonable request from the corresponding authors.

ORCID

Sabah Mozafari https://orcid.org/0000-0002-8166-2465
Tanja Kuhlmann https://orcid.org/0000-0002-0174-5042

Gianvito Martino https://orcid.org/0000-0003-1295-9131
Anne Baron-Van Evercooren https://orcid.org/0000-0002-4150-2205

REFERENCES

Altevogt, B. M., & Paul, D. L. (2004). Four classes of intercellular channels between glial cells in the CNS. *The Journal of Neuroscience*, *24*(18), 4313–4323. https://doi.org/10.1523/JNEUROSCI.3303-03.2004

Basu, R., Bose, A., Thomas, D., & Das Sarma, J. (2017). Microtubule-assisted altered trafficking of astrocytic gap junction protein connexin 43 is associated with depletion of connexin 47 during mouse hepatitis virus infection. *The Journal of Biological Chemistry*, *292*(36), 14747–14763. https://doi.org/10.1074/jbc.M117.786491

Basu, R., & Sarma, J. D. (2018). Connexin 43/47 channels are important for astrocyte/oligodendrocyte cross-talk in myelination and demyelination. *Journal of Biosciences*, *43*(5), 1055–1068.

Blanchard, B., Heurtaux, T., Garcia, C., Moll, N. M., Caillava, C., Grandbarbe, L., … Nait Oumesmar, B. (2013). Tocopherol derivative TFA-12 promotes myelin repair in experimental models of multiple sclerosis. *The Journal of Neuroscience*, *33*(28), 11633–11642. https://doi.org/10.1523/JNEUROSCI.0774-13.2013

Brand-Schieber, E., Werner, P., Iacobas, D. A., Iacobas, S., Beelitz, M., Lowery, S. L., … Scemes, E. (2005). Connexin43, the major gap junction protein of astrocytes, is down-regulated in inflamed white matter in an animal model of multiple sclerosis. *Journal of Neuroscience Research*, *80*(6), 798–808. https://doi.org/10.1002/jnr.20474

Buchet, D., Garcia, C., Deboux, C., Nait-Oumesmar, B., & Baron-Van Evercooren, A. (2011). Human neural progenitors from different foetal forebrain regions remyelinate the adult mouse spinal cord. *Brain*, *134*(Pt 4), 1168–1183. https://doi.org/10.1093/brain/awr030

Chanoumidou, K., Mozafari, S., Baron-Van Evercooren, A., & Kuhlmann, T. (2020). Stem cell derived oligodendrocytes to study myelin diseases. *Glia*, *68*(4), 705–720. https://doi.org/10.1002/glia.23733

Claycomb, K. I., Johnson, K. M., Winokur, P. N., Sacino, A. V., & Crocker, S. J. (2013). Astrocyte regulation of CNS inflammation and remyelination. *Brain Sciences*, *3*(3), 1109–1127. https://doi.org/10.3390/brainsci3031109

Cotrina, M. L., & Nedergaard, M. (2012). Brain connexins in demyelinating diseases: Therapeutic potential of glial targets. *Brain Research*, *1487*, 61–68. https://doi.org/10.1016/j.brainres.2012.07.003

Deboux, C., Ladraa, S., Cazaubon, S., Ghribi-Mallah, S., Weiss, N., Chaverot, N., … Baron-Van Evercooren, A. (2013). Overexpression of CD44 in neural precursor cells improves trans-endothelial migration and facilitates their invasion of perivascular tissues in vivo. *PLoS One*, *8*(2), e57430. https://doi.org/10.1371/journal.pone.0057430

Ehrlich, M., Mozafari, S., Glatza, M., Starost, L., Velychko, S., Hallmann, A. L., … Kuhlmann, T. (2017). Rapid and efficient generation of oligodendrocytes from human induced pluripotent stem cells using transcription factors. *Proceedings of the National Academy of Sciences of the United States of America*, *114*(11), E2243–E2252. https://doi.org/10.1073/pnas.1614412114

Fasciani, I., Pluta, P., Gonzalez-Nieto, D., Martinez-Montero, P., Molano, J., Paino, C. L., … Barrio, L. C. (2018). Directional coupling of oligodendrocyte connexin-47 and astrocyte connexin-43 gap junctions. *Glia*, *66*(11), 2340–2352. https://doi.org/10.1002/glia.23471

Giaume, C., Leybaert, L., Naus, C. C., & Saez, J. C. (2013). Connexin and pannexin hemichannels in brain glial cells: Properties, pharmacology, and roles. *Frontiers in Pharmacology*, *4*, 88. https://doi.org/10.3389/fphar.2013.00088

Hirrlinger, J., & Nave, K. A. (2014). Adapting brain metabolism to myelination and long-range signal transduction. *Glia*, *62*(11), 1749–1761. https://doi.org/10.1002/glia.22737

Jaderstad, J., Jaderstad, L. M., Li, J., Chintawar, S., Salto, C., Pandolfo, M., … Herlenius, E. (2010). Communication via gap junctions underlies early functional and beneficial interactions between grafted neural stem cells and the host. *Proceedings of the National Academy of Sciences of the United States of America*, *107*(11), 5184–5189. https://doi.org/10.1073/pnas.0915134107

Kamasawa, N., Sik, A., Morita, M., Yasumura, T., Davidson, K. G., Nagy, J. I., & Rash, J. E. (2005). Connexin-47 and connexin-32 in gap junctions of oligodendrocyte somata, myelin sheaths, paranodal loops and Schmidt-Lanterman incisures: Implications for ionic homeostasis and potassium siphoning. *Neuroscience*, *136*(1), 65–86. https://doi.org/10.1016/j.neuroscience.2005.08.027

Kleopa, K. A., Orthmann, J. L., Enriquez, A., Paul, D. L., & Scherer, S. S. (2004). Unique distributions of the gap junction proteins connexin29, connexin32, and connexin47 in oligodendrocytes. *Glia*, *47*(4), 346–357. https://doi.org/10.1002/glia.20043

Kleopa, K. A., & Scherer, S. S. (2006). Molecular genetics of X-linked Charcot-Marie-Tooth disease. *Neuromolecular Medicine*, *8*(1–2), 107–122. https://doi.org/10.1385/nmm:8:1-2:107

Laterza, C., Merlini, A., de Feo, D., Ruffini, F., Menon, R., Onorati, M., … Martino, G. (2013). iPSC-derived neural precursors exert a neuroprotective role in immune-mediated demyelination via the secretion of LIF. *Nature Communications*, *4*, 2597. https://doi.org/10.1038/ncomms3597

Li, T., Giaume, C., & Xiao, L. (2014). Connexins-mediated glia networking impacts myelination and remyelination in the central nervous system. *Molecular Neurobiology*, *49*(3), 1460–1471. https://doi.org/10.1007/s12035-013-8625-1

Maglione, M., Tress, O., Haas, B., Karram, K., Trotter, J., Willecke, K., & Kettenmann, H. (2010). Oligodendrocytes in mouse corpus callosum are coupled via gap junction channels formed by connexin47 and connexin32. *Glia*, *58*(9), 1104–1117. https://doi.org/10.1002/glia.20991

Markoullis, K., Sargiannidou, I., Gardner, C., Hadjisavvas, A., Reynolds, R., & Kleopa, K. A. (2012). Disruption of oligodendrocyte gap junctions in experimental autoimmune encephalomyelitis. *Glia*, *60*(7), 1053–1066. https://doi.org/10.1002/glia.22334

Markoullis, K., Sargiannidou, I., Schiza, N., Hadjisavvas, A., Roncaroli, F., Reynolds, R., & Kleopa, K. A. (2012). Gap junction pathology in multiple sclerosis lesions and normal-appearing white matter. *Acta Neuropathologica*, *123*(6), 873–886. https://doi.org/10.1007/s00401-012-0978-4

Markoullis, K., Sargiannidou, I., Schiza, N., Roncaroli, F., Reynolds, R., & Kleopa, K. A. (2014). Oligodendrocyte gap junction loss and disconnection from reactive astrocytes in multiple sclerosis gray matter. *Journal of Neuropathology and Experimental Neurology*, *73*(9), 865–879. https://doi.org/10.1097/NEN.0000000000000106

Marteyn, A., Sarrazin, N., Yan, J., Bachelin, C., Deboux, C., Santin, M. D., … Baron-Van Evercooren, A. (2016). Modulation of the innate immune response by human neural precursors prevails over oligodendrocyte progenitor remyelination to rescue a severe model of Pelizaeus-Merzbacher disease. *Stem Cells*, *34*(4), 984–996. https://doi.org/10.1002/stem.2263

Masaki, K. (2015). Early disruption of glial communication via connexin gap junction in multiple sclerosis, Balo's disease and neuromyelitis optica. *Neuropathology*, *35*(5), 469–480. https://doi.org/10.1111/neup.12211

Masaki, K., Suzuki, S. O., Matsushita, T., Matsuoka, T., Imamura, S., Yamasaki, R., … Kira, J. (2013). Connexin 43 astrocytopathy linked to rapidly progressive multiple sclerosis and neuromyelitis optica. *PLoS One*, *8*(8), e72919. https://doi.org/10.1371/journal.pone.0072919

May, D., Tress, O., Seifert, G., & Willecke, K. (2013). Connexin47 protein phosphorylation and stability in oligodendrocytes depend on expression of Connexin43 protein in astrocytes. *The Journal of Neuroscience*, *33*(18), 7985–7996. https://doi.org/10.1523/JNEUROSCI.5874-12.2013

Mozafari S., Baron-Van Evercooren A. (2020). Human stem cell-derived oligodendrocytes: From humanized animal models to cell therapy in

myelin diseases. *Seminars in Cell & Developmental Biology*, https://doi.org/10.1016/j.semcdb.2020.09.011

Mozafari, S., Laterza, C., Roussel, D., Bachelin, C., Marteyn, A., Deboux, C., … Baron-Van Evercooren, A. (2015). Skin-derived neural precursors competitively generate functional myelin in adult demyelinated mice. *The Journal of Clinical Investigation*, *125*(9), 3642–3656. https://doi.org/10.1172/JCI80437

Mozafari S., Starost L., Manot-Saillet B., Garcia-Diaz B., Xu Y. K. T., Roussel D., … Evercooren A. B.-V. (2020). Multiple sclerosis iPS-derived oligodendroglia conserve their properties to functionally interact with axons and glia in vivo. *Science Advances*, *6*(49), eabc6983. https://doi.org/10.1126/sciadv.abc6983

Nagy, J. I., Ionescu, A. V., Lynn, B. D., & Rash, J. E. (2003). Coupling of astrocyte connexins Cx26, Cx30, Cx43 to oligodendrocyte Cx29, Cx32, Cx47: Implications from normal and connexin32 knockout mice. *Glia*, *44*(3), 205–218. https://doi.org/10.1002/glia.10278

Odermatt, B., Wellershaus, K., Wallraff, A., Seifert, G., Degen, J., Euwens, C., … Willecke, K. (2003). Connexin 47 (Cx47)-deficient mice with enhanced green fluorescent protein reporter gene reveal predominant oligodendrocytic expression of Cx47 and display vacuolized myelin in the CNS. *The Journal of Neuroscience*, *23*(11), 4549–4559.

Orthmann-Murphy, J. L., Abrams, C. K., & Scherer, S. S. (2008). Gap junctions couple astrocytes and oligodendrocytes. *Journal of Molecular Neuroscience*, *35*(1), 101–116. https://doi.org/10.1007/s12031-007-9027-5

Ottoboni, L., von Wunster, B., & Martino, G. (2020). Therapeutic plasticity of neural stem cells. *Frontiers in Neurology*, *11*, 148. https://doi.org/10.3389/fneur.2020.00148

Ozog, M. A., Bernier, S. M., Bates, D. C., Chatterjee, B., Lo, C. W., & Naus, C. C. (2004). The complex of ciliary neurotrophic factor-ciliary neurotrophic factor receptor alpha up-regulates connexin43 and intercellular coupling in astrocytes via the Janus tyrosine kinase/signal transducer and activator of transcription pathway. *Molecular Biology of the Cell*, *15*(11), 4761–4774. https://doi.org/10.1091/mbc.e04-03-0271

Parenti, R., Cicirata, F., Zappala, A., Catania, A., la Delia, F., Cicirata, V., … Willecke, K. (2010). Dynamic expression of Cx47 in mouse brain development and in the cuprizone model of myelin plasticity. *Glia*, *58*(13), 1594–1609. https://doi.org/10.1002/glia.21032

Pluchino, S., Smith, J. A., & Peruzzotti-Jametti, L. (2020). Promises and limitations of neural stem cell therapies for progressive multiple sclerosis. *Trends in Molecular Medicine*, *26*, 898–912. https://doi.org/10.1016/j.molmed.2020.04.005

Rash, J. E. (2010). Molecular disruptions of the panglial syncytium block potassium siphoning and axonal saltatory conduction: Pertinence to neuromyelitis optica and other demyelinating diseases of the central nervous system. *Neuroscience*, *168*(4), 982–1008. https://doi.org/10.1016/j.neuroscience.2009.10.028

Reinhardt, P., Glatza, M., Hemmer, K., Tsytsyura, Y., Thiel, C. S., Hoing, S., … Sterneckert, J. (2013). Derivation and expansion using only small molecules of human neural progenitors for neurodegenerative disease modeling. *PLoS One*, *8*(3), e59252.

Shinkai, Y. (1992). RAG-2-deficient mice lack mature lymphocytes owing to inability to initiate V(D)J rearrangement. *Cell*, *68*(5), 855–867. https://doi.org/10.1016/0092-8674(92)90029-c

Theotokis, P., Kleopa, K. A., Touloumi, O., Lagoudaki, R., Lourbopoulos, A., Nousiopoulou, E., … Grigoriadis, N. (2015). Connexin43 and connexin47 alterations after neural precursor cells transplantation in experimental autoimmune encephalomyelitis. *Glia*, *63*(10), 1772–1783. https://doi.org/10.1002/glia.22843

Tress, O., Maglione, M., May, D., Pivneva, T., Richter, N., Seyfarth, J., … Willecke, K. (2012). Panglial gap junctional communication is essential for maintenance of myelin in the CNS. *The Journal of Neuroscience*, *32*(22), 7499–7518. https://doi.org/10.1523/JNEUROSCI.0392-12.2012

Uhlenberg, B., Schuelke, M., Ruschendorf, F., Ruf, N., Kaindl, A. M., Henneke, M., … Gartner, J. (2004). Mutations in the gene encoding gap junction protein alpha 12 (connexin 46.6) cause Pelizaeus-Merzbacher-like disease. *American Journal of Human Genetics*, *75*(2), 251–260. https://doi.org/10.1086/422763

Xia, C. Y., Xu, J. K., Pan, C. H., Lian, W. W., Yan, Y., Ma, B. Z., … Zhang, W. K. (2020). Connexins in oligodendrocytes and astrocytes: Possible factors for demyelination in multiple sclerosis. *Neurochemistry International*, *136*, 104731. https://doi.org/10.1016/j.neuint.2020.104731

Zhao, Y., Yamasaki, R., Yamaguchi, H., Nagata, S., Une, H., Cui, Y., … Kira, J. I. (2020). Oligodendroglial connexin 47 regulates neuroinflammation upon autoimmune demyelination in a novel mouse model of multiple sclerosis. *Proceedings of the National Academy of Sciences of the United States of America*, *117*(4), 2160–2169. https://doi.org/10.1073/pnas.1901294117

SUPPORTING INFORMATION

Additional supporting information may be found online in the Supporting Information section at the end of this article.

How to cite this article: Mozafari S, Deboux C, Laterza C, et al. Beneficial contribution of induced pluripotent stem cell-progeny to Connexin 47 dynamics during demyelination-remyelination. *Glia*. 2021;69:1094–1109. https://doi.org/10.1002/glia.23950